processes

Article

Numerical Analysis of Heat Transfer Enhancement Due to Nanoparticles under the Magnetic Field in a Solar-Driven Hydrothermal Pretreatment System

Yang Yu *, Kai Wang, Yurong Zhao *, Qicheng Chen and Nanhang Dong

School of Energy and Power Engineering, Northeast Electric Power University, Jilin 132012, China
* Correspondence: yangyu@neepu.edu.cn (Y.Y.); yrzhao@neepu.edu.cn (Y.Z.)

Abstract: Solar-driven hydrothermal pretreatment is an efficient approach for the pretreatment of microalgae biomass for biofuel production. In order to enhance the heat transfer, the magnetic fields effects on flow and heat transfer of nanofluids were investigated in a three-dimensional circular pipe. The magnetic fields were applied in different directions and magnetic field intensities to the flow. In this paper, Finite Volume Method was used to simulate flow and heat transfer of nanofluids under a magnetic field, and the Discrete Phase Model was selected to calculate two-phase flow, which was water mixed with metal nanoparticles. The research was also carried out with the various physical properties of nanoparticles, including the volume share of nanoparticles, particle diameter, and particle types. When the magnetic fields were applied along the X, Y, and Z directions and the intensity of magnetic fields was 0.5 T, the heat transfer coefficients of Cu-H_2O nanofluids flow were increased evenly by 9.17%, 10.28%, and 10.32%, respectively. When the magnetic field was applied, the heat transfer coefficients and the Nusselt numbers were both increased with the increment of intensities of the magnetic field.

Keywords: nanofluids; heat transfer enhancement; magnetic field; microalgae; numerical simulation

Citation: Yu, Y.; Wang, K.; Zhao, Y.; Chen, Q.; Dong, N. Numerical Analysis of Heat Transfer Enhancement Due to Nanoparticles under the Magnetic Field in a Solar-Driven Hydrothermal Pretreatment System. *Processes* **2022**, *10*, 2649. https://doi.org/10.3390/pr10122649

Academic Editor: Karakasidis Theodoros

Received: 20 November 2022
Accepted: 6 December 2022
Published: 9 December 2022

1. Introduction

The current situation of increasingly prominent energy issues and continuous demand has attracted worldwide attention under the premise of rapid economic development. In the solar-driven hydrothermal pretreatment system, microalgae slurry directly flowed through a parabolic trough collector and absorbed solar energy for pretreatment [1], heat transfer often occurs during production operation, and the effective use of energy is extremely critical. A very advanced and efficient heat transfer technology is needed to improve heat transfer performance and heat transfer efficiency. Next, production load and heat transfer intensity increase in the use of heat exchange equipment [2–4]. Therefore, from the perspective of heat transfer materials and working fluids, we are looking for and developing more excellent materials and working fluids to improve fluid thermal conductivity [5–8] in order to enhance the ability of heat transfer. As a new type of working fluid, nanofluids [9] have a strong heat transfer performance, so they are used in many scientific and technological fields such as electronics, aerospace, machinery, medical treatment, etc. [10–14]. In the energy fields such as solar power generation, solar collectors, nuclear energy, and renewable energy [15–18], nanofluids have also been widely used.

The research on nanofluids has very important scientific and application significance. It opens up a new direction for people to explore the field of fluid heat transfer, and greatly promotes the innovation and development of nanotechnology. The development of nanofluids originated from Choi [19], who first introduced the concept of "nanofluids" in the U.S. National Laboratory in 1995. Researchers in the laboratory measured the thermal conductivity of nanofluids through experiments and concluded that nanoparticles were added. After that, the thermal conductivity of the fluid can be significantly enhanced.

Since then, nanofluids have gradually entered people's field of vision and have achieved relatively rapid development. Wang et al. [20] proposed a fractal model to predict the effective thermal conductivity of non-metallic nanoparticle dilute suspensions in 2003. It involved the application and improvement of effective media theory. The proposed fractal model predicted the dilution of nanoparticles well and predicted the change trend of effective thermal conductivity. When the volume fraction is less than 0.5%, the experimental data of adding 50 nm CuO suspended particles in deionized water was successfully fitted. The calculation results also showed that the thermal conductivity of the fluid with the nanoparticle suspension was better than that of the deionized water-based fluid. Sun [21] studied the flow and heat transfer characteristics of Cu-H_2O nanofluids with built-in twisted ribbon tube, and the results showed that the Nusselt numbers of Cu-H_2O nanofluids increased with the increments of Reynolds numbers and volume fraction φ. When the volume fraction was φ = 0.5%, the enhancement range of Cu-H_2O nanofluids in the built-in twisted ribbon tube with torsion ratio Y = 3.5 and Y = 5.5 were 2.29 and 2.14, respectively. İlhan et al. [22] conducted an experimental study on hexagonal boron nitride nanofluids and found that its thermal conductivity was significantly higher than that of the base fluid. In addition, the thermal conductivity of the water-based hexagonal boron nitride nanofluids with relatively dilute particle suspensions increases significantly with the increase of its viscosity. Karthikeyan [23] studied the effect of physical properties on the thermal conductivity of nanofluids and found that the size, polydispersity, particle agglomeration, and the volume fraction of nanoparticles in the suspension have a significant effect on the thermal conductivity of the suspension.

Recently, the thermal energy transportation of nanofluids was studied, especially in micro/nano scale. The utilization of nanofluids in micro/nano scale heat were not hitherto summarized but mass transfer fields were summarized, especially for some chemistry relating applications, and nanofluids were also able to offer insights for novel micro/nano scale energy transportation [24]. Liu et al. [25] summarized the characteristics and applications of glycerol and its derivatives as functional media for energy transportation and reviewed the preparation and modification strategies for nanomaterial synthesis. The applications of these fluids in industrial process were also discussed systematically. Furthermore, advantages and drawbacks of glycerol in energy transportation were concluded. Deep eutectic solvents (DESs) are a new type of ionic liquid alternatives, usually composed of a certain stoichiometric ratio of hydrogen bond acceptors and hydrogen bond donors via hydrogen bonding association. Liu et al. [26] developed a novel "one-step" preparation protocol using $Cu(OH)_2$ as a precursor and deep eutectic solvents (DESs) as dispersing medium, in order to solve the poor stability associated with short liquid range of traditional nanofluids. The as-prepared nanofluid bears an extraordinary static stability that can be kept for at least two months without observation of any sedimentation thanks to the in-situ formed Cu_2O nanoparticle in DESs under a microwave irradiation condition and wide liquid range attributed to the low saturated pressure of DESs. Glycerol/choline chloride (ChCl) DES based nanofluids were prepared by dispersion of nano-TiO_2, Fe_2O_3, CuO, SiC and carbon. Viscosity and thermal conductivity (TC) were studied comprehensively as functions of testing temperature and mass fraction. The highest thermal conductivity was found to be increased by up to 4.23%. More importantly, specific heat capacity, the other key factor in energy transportation for working fluids, was studied with respect to that of nano-additive and temperature, which indicates that it could be effectively increased by 26.23% compared to that of pristine base solvent [27].

Magnetic fields are crucial in the non-intrusive flow control of electrically conducting melts in various physics of industrial significance. Magnetic fields can affect the flow with electrically conducting materials and enhance the heat transfer. Bahiraei et al. [28] studied the cooling effect of magnetic nanofluids as a coolant on a double-tube heat exchanger under the action of a magnetic field and studied the effect of a quadrupole magnetic field on a countercurrent double-tube heat exchanger using the Euler Lagrangian method. The influence of the cooling performance of the nanofluids was discussed. The results

showed that the applied magnetic field increases the pressure drop and enhances the heat transfer effect. This phenomenon was more obvious at lower Reynolds numbers. At the same time, the effect of magnetic force makes the particle concentration distribution on the tube section more uniform. Naphon et al. [29] conducted an experimental study on the laminar flow and heat transfer of nanofluids in micro-finned tubes under the action of a magnetic field, and studied the effects of pulsating flow, micro-finned tube, and magnetic field combined enhanced heat transfer technology on the nanofluids flow and heat transfer in micro-finned tubes. The results showed that the Nusselt number of the nanofluids under the action of a magnetic field was 6.23% higher than that without a magnetic field. When the magnetic field frequency was 20 Hz, the Nusselt number of the nanofluids was 22.21% higher than that of the pure water working fluid. Hajmohammadi et al. [30] used the single-phase method and the two-phase method to study the flow and heat transfer characteristics of nanofluids between two cylinders under the action of a magnetic field. The results showed that the effect of the magnetic field was greater than that of the volume fraction of nanoparticles and other parameters on heat transfer. As a result, the addition of the magnetic field greatly reduced the shear stress of the outer ring and enhances the heat transfer performance of the nanofluids between the cylinders. Selimefendigila and F.Öztop [31] combined utilization of an elastic fin and magnetic field on the phase change process dynamics, and numerically assessed during nanoliquid convection in a phase change material (PCM)-packed bed embedded cylindrical reactor. Elastic fin with radially acting magnetic field provides an excellent contribution for controlling the phase change dynamics in a PCM-installed cylindrical reactor. In the paper [32], the mechanism, influencing factors, and influencing laws of magnetic field enhanced heat transfer of nanofluids are reviewed, and the application of a magnetic field to heat transfer of nanofluids is also briefly summarized. For the direction of the magnetic field, enhancing heat transfer is the most crucial problem to be considered by researchers in the future. As the review of the pertinent literature, it indicates that there were many papers presented that studied heat transfer characteristics of nanofluids with and without magnetic field effect. However, there was no research paper that reported the effect of magnetic field strength on heat transfer characteristics of nanofluids and there was still room for discussion, especially on the effect of different directions of the magnetic field. Therefore, the objective of this paper was to study heat transfer enhancement for solar-driven hydrothermal pretreatment system by nanoparticles under the magnetic field. The Cu-H_2O and Al-H_2O nanofluids flow through the high-temperature pipe under the magnetic fields were established. The influence of the diameters and the volume fractions of nanoparticles on the flow and heat transfer of the nanofluids were analyzed. Next, the effect different directions and intensities of the magnetic field on the nanofluids flow were discussed.

2. Physical Model and Numerical Method

2.1. Physical Model

Figure 1a illustrated the geometry of flow and heat transfer of nanofluids. The three-dimensional round pipe is divided into three sections, and the distance of each section is equal. Each section of circular pipe is 550 mm long, 100 mm in diameter, and the angle between each section of circular pipe is 90 degrees. In order to analyze how the direction of the magnetic field enhances heat transfer of nanofluids flow, there are sections along X, Y, and Z directions, respectively. The selected inlet section that took the direction of the fluid flowing in the pipe was the Z direction, the direction perpendicular to outlet was the Y direction and the other direction was the X direction. When the mathematical model was established, the assumptions were made as follows:

(1) The flows of nanofluids were quasi-steady state turbulent;
(2) The internal heat exchange only exists between the fluid and the wall, and there is no radiation heat exchange phenomenon;

(3) The influence of internal flow field and external interference factors were ignored, such as the influence of ambient temperature and atmospheric pressure.

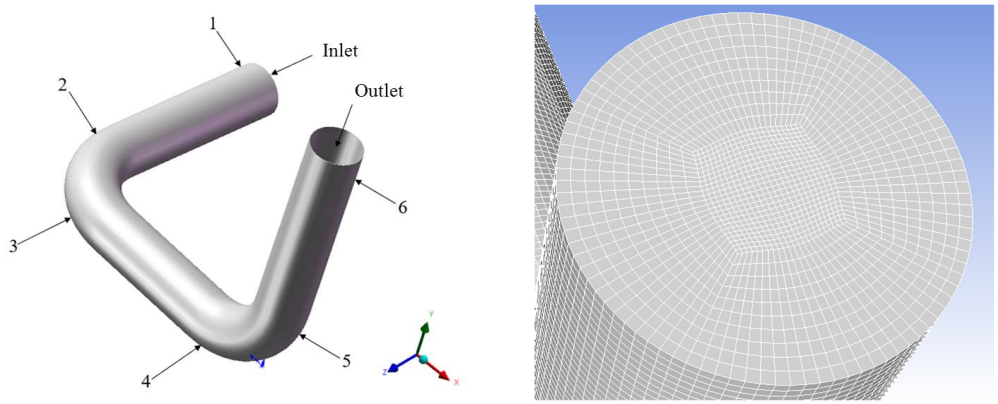

(**a**) (**b**)

Figure 1. (**a**) The geometry of three-dimensional circular pipe in which the nanofluids flow under a uniform magnetic field. 1 is inlet and 6 is outlet, 2, 3, 4, and 5 are the faces in the pipe. (**b**) Grid distribution on the outlet.

2.2. Numerical Method

The control equations of the flow and heat transfer of nanofluids are as follows:

$$\frac{\partial \rho}{\partial t} + \frac{\partial}{\partial x}(\rho u) + \frac{\partial}{\partial y}(\rho v) + \frac{\partial}{\partial z}(\rho w) = 0 \quad (1)$$

$$u\frac{\partial u}{\partial x} + v\frac{\partial u}{\partial y} + w\frac{\partial u}{\partial z} + F_m = -\frac{1}{\rho}\frac{\partial p}{\partial x} + \frac{\mu}{\rho}\left(\frac{\partial^2 u}{\partial x^2} + \frac{\partial^2 u}{\partial y^2} + \frac{\partial^2 u}{\partial z^2}\right) + \frac{B_0^2}{\mu}\left(\frac{\partial^2 u}{\partial x^2} + \frac{\partial^2 u}{\partial y^2} + \frac{\partial^2 u}{\partial z^2}\right) \quad (2)$$

$$u\frac{\partial v}{\partial x} + v\frac{\partial v}{\partial y} + w\frac{\partial v}{\partial z} + F_m = -\frac{1}{\rho}\frac{\partial p}{\partial y} + \frac{\mu}{\rho}\left(\frac{\partial^2 v}{\partial x^2} + \frac{\partial^2 v}{\partial y^2} + \frac{\partial^2 v}{\partial z^2}\right) + \frac{B_0^2}{\mu}\left(\frac{\partial^2 v}{\partial x^2} + \frac{\partial^2 v}{\partial y^2} + \frac{\partial^2 v}{\partial z^2}\right) \quad (3)$$

$$u\frac{\partial w}{\partial x} + v\frac{\partial w}{\partial y} + w\frac{\partial w}{\partial z} + F_m = -\frac{1}{\rho}\frac{\partial p}{\partial z} + \frac{\mu}{\rho}\left(\frac{\partial^2 w}{\partial x^2} + \frac{\partial^2 w}{\partial y^2} + \frac{\partial^2 w}{\partial z^2}\right) + \frac{B_0^2}{\mu}\left(\frac{\partial^2 w}{\partial x^2} + \frac{\partial^2 w}{\partial y^2} + \frac{\partial^2 w}{\partial z^2}\right) \quad (4)$$

$$u\frac{\partial T}{\partial x} + v\frac{\partial T}{\partial y} + w\frac{\partial T}{\partial z} = \frac{\lambda}{\rho c_p}\frac{\partial^2 T}{\partial x^2} + \frac{\lambda}{\rho c_p}\frac{\partial^2 T}{\partial y^2} + \frac{\lambda}{\rho c_p}\frac{\partial^2 T}{\partial z^2} \quad (5)$$

where u, v, w are the velocity components in the x, y, and z directions, ρ is the density of the nanofluids, p is the pressure, B_0 is the magnitude of the magnetic field, F_m is the magnitude of the magnetic field force, μ is the kinematic viscosity of the nanofluids, c_p is the specific heat at constant pressure of the nanofluids, and T is the wall temperature.

The numerical method in this paper is the finite volume method, and the k-εmodel was selected to simulate the turbulent flow and heat transfer of nanofluids. The two-phase flows of nanofluids were mixed with water and metal nanoparticles, and the Discrete Phase Mode (DPM) was selected to simulate the two-phase flows because the volume fractions of nanofluids are less than 2% in this paper. When the equations were solved, the velocity inlet was set as the inlet and the pressure outlet was set as the outlet. The inlet temperature of the nanofluids was set as 293 K, and the temperature of the wall was set at a high temperature of 363 K. The pipe wall was set as the non-slip boundary condition, and the vertical pipe was subjected to a uniform magnetic field. As shown in Figure 1b, the structured grid was chosen when the pipe was meshed. After non-correlation analysis for grids, when the number of grids reached 0.56 million, the results had little variation.

3. Numerical Results and Discussions

In this paper, the magnetic fields effects on flow and heat transfer of Cu-H_2O and Al-H_2O nanofluids flow were investigated. The diameters of nanoparticles were chosen as 100 nm, 200 nm, and 500 nm, and the volume fractions of nanoparticles were chosen as 0.5%, 1%, and 2%. The physical parameters of various materials are shown in Table 1. This study was carried out from two aspects, namely the direction of the magnetic field and different magnetic field strengths on the flow heat transfer of Cu-H_2O and Al-H_2O nanofluids. influence of characteristics. Two parameters, convective heat transfer coefficient and Nusselt number, were used for analyzing the influence of volume fraction on the flow and heat transfer of nanofluids. In this paper, the convective heat transfer coefficient and Nusselt number were calculated as follows:

$$h_{ave} = \frac{Q}{A_c \Delta T_m} \tag{6}$$

$$Nu = \frac{h_{ave} D_h}{\lambda} \tag{7}$$

where Q is the total heat exchange in this system, A_c is the total heat exchange area of the circular tube, ΔT_m is the temperature difference between the nanofluids and the isothermal wall, and λ is the thermal conductivity of nanofluids. The calculation formula of temperature difference ΔT_m and total heat exchange Q is as follows:

$$\Delta T_m = T_w - \frac{1}{2}(T_{in} + T_{out}) \tag{8}$$

$$Q = C_p q_m (T_{out} - T_{in}) \tag{9}$$

where T_w is the temperature of the heating wall, T_{in} is the inlet inflow temperature of the nano fluids flow, T_{out} is the outlet outflow temperature, and q_m is the mass flow rate of the nanofluids.

Table 1. Material property parameters [12].

Physical Parameters	Calculated Value	Unit
Diameters of Cu nanoparticle	100/200/500	nm
Density of Cu nanoparticle	8900	kg/m^3
Volume fractions of the nanofluids	0.5/1.0/2.0	%vol
Viscosity of Cu-H_2O nanofluids	$(1.14/1.17/1.20) \times 10^{-3}$	$m^2 \cdot s^{-1}$
Density of Cu-H_2O nanofluids	1032.718/1056.918/1087.636	kg/m^3
Diameters of Al nanoparticle	100/200/500	Nm
Density of Al nanoparticle	2700	kg/m^3
Volume fractions of the nanofluids	0.5/1.0/2.0	%vol
Viscosity of Al-H_2O nanofluids	$(1.04/1.05/1.06) \times 10^{-3}$	$m^2 \cdot s^{-1}$
Density of Al-H_2O nanofluids	1006.512/1015.023/1032.041	kg/m^3
Density of Pure water	1000	kg/m^3
Pure water viscosity	100.3×10^{-5}	$m^2 \cdot s^{-1}$

3.1. Validations

In order to verify the reliability and accuracy of the numerical simulation method, the same numerical simulation method was used to simulate the flows of pure water and nanofluids. The numerical simulation results were compared with the results calculated by the empirical correlation formula of turbulent flow and heat transfer [33], as shown in Figure 2a. It was shown that the maximum deviation between the results of the numerical simulation and the empirical correlation formula was within ±20%, indicating that the numerical simulation method was reliable and accurate. The numerical simulation results also were compared with the experimental results of Xuan [34] and the simulation results of Bennia [35]. In Figure 2b, the Nusselt value of the nanofluids simulated by the

numerical method was almost the same as Xuan's experimental result, and the maximum error was 3.6%. The maximum error was 5% compared with Bennia's simulation results. The two comparisons indicated that the numerical simulation method was reliable and accurate again.

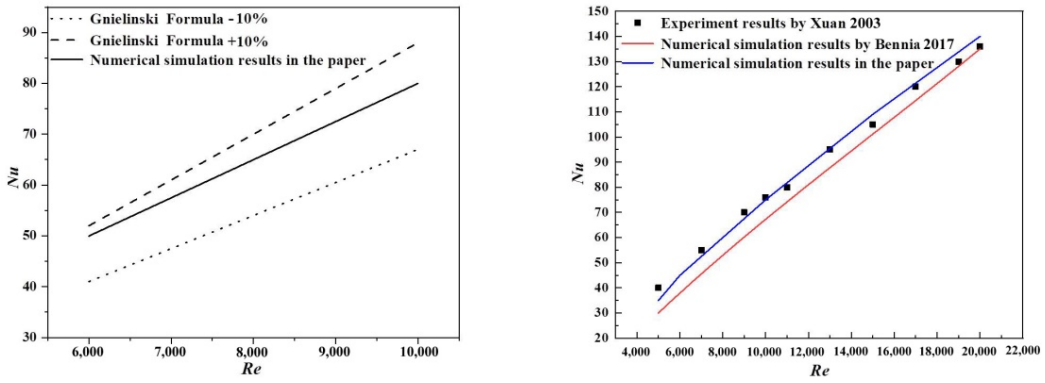

(**a**) (**b**)

Figure 2. The comparisons between the numerical simulation results and other results. (**a**) Gnielinski formula calculation on pure water flow, (**b**) Xuan's experimental results [34], and Bennia's simulation results [35].

3.2. Results and Discussions without Magnetic Effect

The diameters of the Cu and Al nanoparticles were 100 nm, and the volume fractions of the nanofluids were 0.5%, 1%, and 2%. The effects of three different intensities of magnetic fields, 0.2 T, 0.5 T, and 0.8 T, on the forced convective heat transfer of the nanofluids flow in the pipe were studied.

Figure 3 illustrated that the heat transfer coefficients of Cu-H_2O nanofluids flow varied with different Reynolds numbers in the pipe. In Figure 3a, the particle size was 500 nm. When the volume fraction of nanoparticle increased 1%, the convective heat transfer coefficient increased by about 6.73%. In Figure 3b, the particle size was 200 nm. When the volume fraction of nanoparticle increased 1%, the convective heat transfer coefficient increased by about 9.25%. In Figure 3c, the particle size was 100 nm. When the volume fraction of nanoparticle increased 1%, the convective heat transfer coefficient increased by about 14.86%. These results indicated that, in the flow of nanofluids at a low volume fraction of nanoparticle, the larger the volume fraction, the greater the convective heat transfer coefficient of the nanofluids. When the volume fraction of nanoparticles was increased, it meant that the concentration of nanoparticles increased. Finally, the convective heat transfer coefficient was increased, and the convective heat transfer capacity of the flow was enhanced. The heat transfer coefficient of the nanofluids flow gradually increased as the particle diameter decreased. Therefore, it was concluded that, as the size of nanoparticles gradually decreased, the heat transfer capabilities of nanofluids increased. It was also summarized that the larger the volume fraction, the greater the convective heat transfer coefficient of the nanofluids. Taking the smallest particle size as an example, when the volume fraction of nanoparticle was 0.5%, the convective heat transfer coefficient increased by about 8.21%, larger than pure water. When the volume fraction of nanoparticle was 1%, the convective heat transfer coefficient increased by about 15.23% larger than pure water. When the volume fraction of nanoparticle was 2%, the convective heat transfer coefficient increased by about 28.52% larger than pure water.

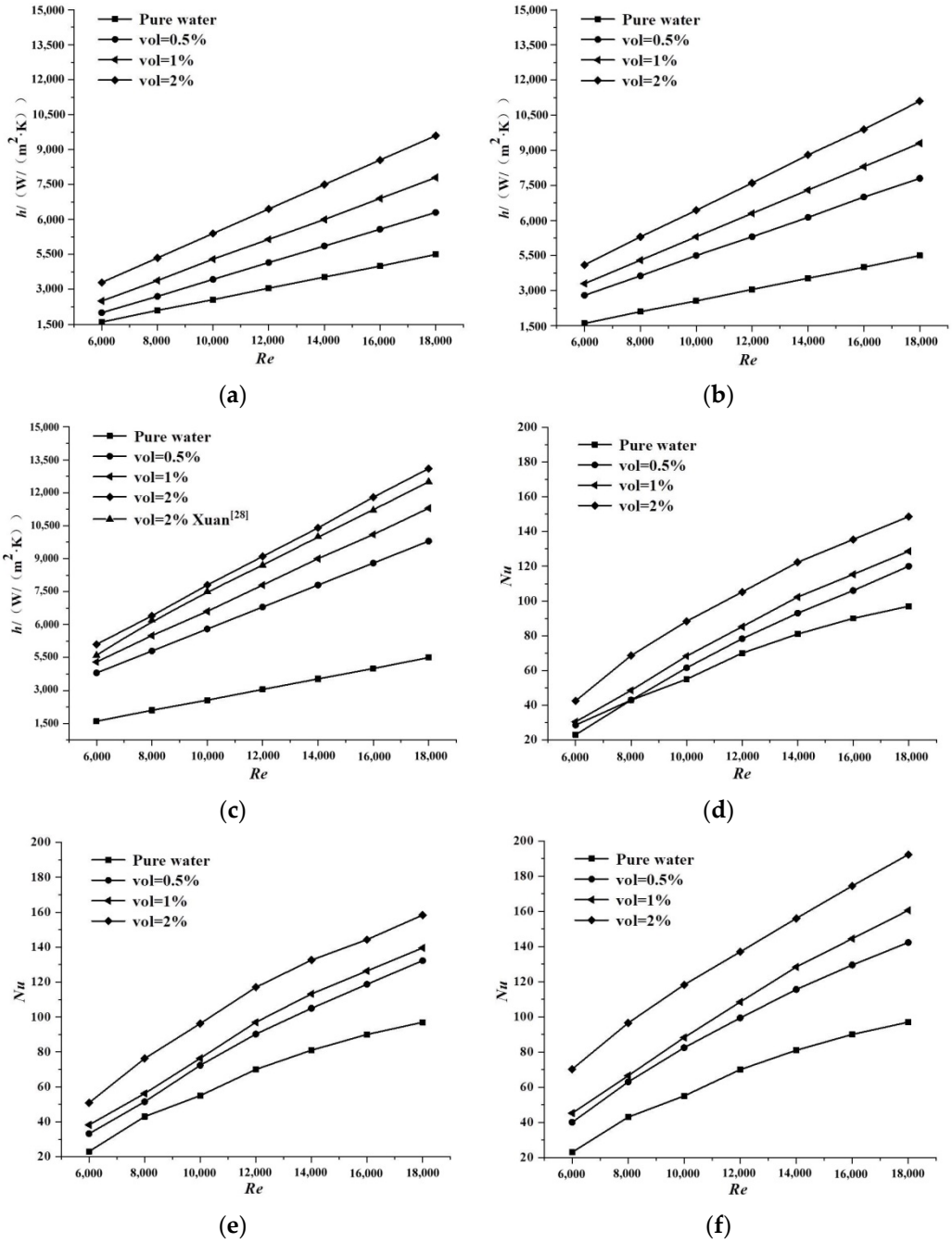

Figure 3. The heat transfer coefficients and Nusselt numbers of Cu-H_2O nanofluids flow varied with different Reynolds numbers. The diameters of particle were 500 nm (**a**,**d**), 200 nm (**b**,**e**), and 100 nm (**c**,**f**).

In Figure 3d–f, the Nusselt numbers of nanofluids flow varied with different Reynolds numbers when the nanoparticles sizes were 100 nm, 200 nm, and 500 nm, and the volume fractions of nanoparticles were 0.5%, 1%, and 2%. The Nusselt number of the nanofluids flow gradually increased as the particle diameter decreased when the volume fraction of nanoparticles was fixed. When the volume fraction of nanoparticles was 2%, the Nusselt number of the nanofluids flow was about 9.2% larger than which of pure water. The Nusselt number of the 200 nm nanofluids flow was about 15.7% larger than which of pure water, and the Nusselt number of the 100 nm nanofluids flow was increased by about 26.3% compared to pure water. Under the condition of the same particle diameter, the volume fractions of nanoparticles affected the change of the Nusselt numbers, which in

turn affected the heat transfer capacity of the nanofluids flow. The larger the volume fraction, the more it can collide with surrounding molecules during the nanofluids flow, and the larger rate of energy exchange speeds up accordingly. Thus, it strengthened the heat transfer capability of the nanofluids flow, and indirectly enhanced the heat transfer capability between the nanofluids and the external environment.

3.3. Results and Discussions for Different Directions of Magnetic Field

In the paper, the effect of magnetic field on the heat transfer of the nanofluids flow was considered, and the magnetic fields were applied along the X, Y, and Z directions, respectively. As Figure 1a shows, by calculating the temperature distribution on six faces, the influences of the magnetic field on the flow were first explored. Faces 1 and 6 are the inlet and outlet. Face 2 is the end of the first section when it is not bending. Faces 3 and 4 are the beginning and end of the second section. Face 5 is the beginning of the third section.

In Figure 4, when the magnetic fields were applied along the X direction, the temperature distributions of Cu-H_2O and Al-H_2O nanofluids flow were illustrated along the diameter on faces 2, 3, 4, 5, and 6, respectively. It was shown that the nanoparticles in the nanofluids flow were disturbed by the Lorentz force from the inlet. The temperature distributions with or without the magnetic field were obvious. Although the flows in the middle section were not affected by the X direction magnetic field, the temperature differences formed in the entrance part were maintained. As shown in Figure 4d,e, because the Lorentz force continued to act on the nanoparticles in the exit section, the temperatures in the nanofluids flow under the action of the magnetic field rose faster.

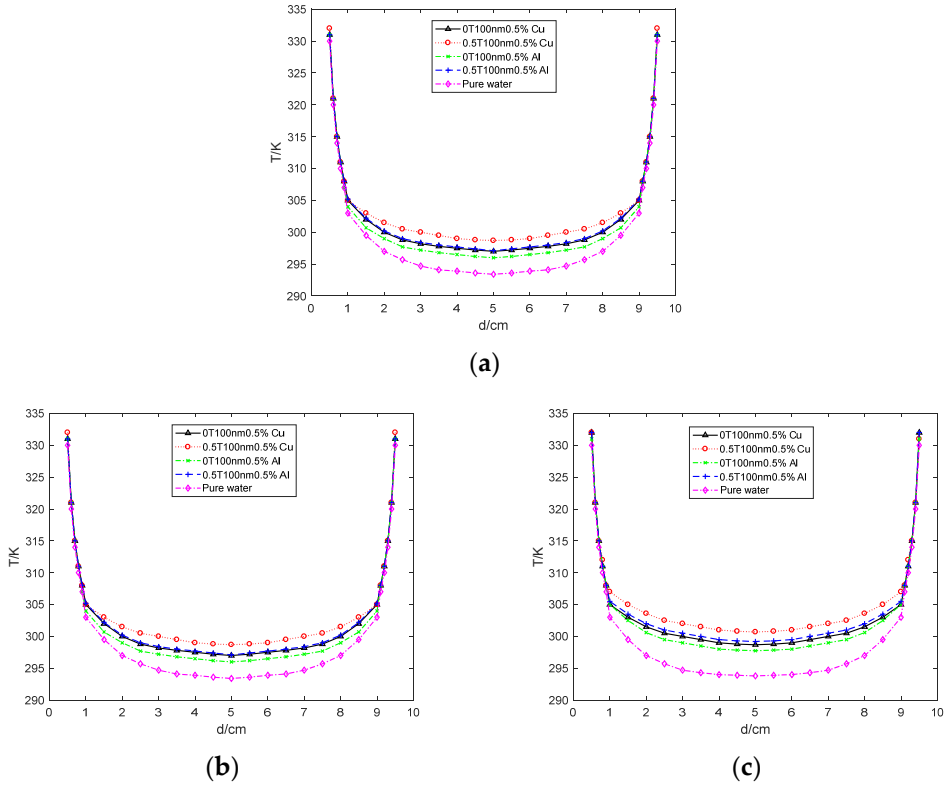

Figure 4. *Cont.*

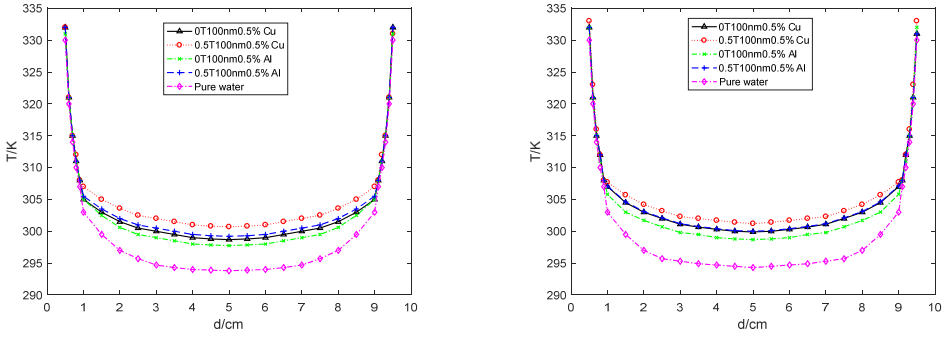

Figure 4. The temperature distributions of Cu-H_2O and Al-H_2O nanofluids flow along the diameter on faces 2 (**a**), 3 (**b**), 4 (**c**), 5 (**d**), and 6 (**e**), respectively. The magnetic fields were applied along the X direction.

Figure 5 showed that the temperature distributions of Cu-H_2O and Al-H_2O nanofluids flow were illustrated along the diameter on faces 2, 3, 4, 5, and 6, respectively, when the magnetic fields were applied along the Z direction. Since the direction of nanofluids flow in the inlet section was the same as the direction of the magnetic field of induction, no Lorenz force was generated. Then the magnetic field had almost no effect on the nanofluids flow, as shown in Figure 5a. In Figure 5b, the temperature of the nanofluids flow on face 3 had a little increment and was initially subjected to the magnetic field. While the nanofluids flow was in the middle and the outlet sections, the nanoparticles in the nanofluids were disturbed under the action of the magnetic field, and the flow and heat transfer behavior of the nanofluids flow had changed. Therefore, the temperatures of the nanofluid flow on faces 4, 5, and 6 were more obviously increased. When the magnetic fields were applied along the Y direction, the influences were similar with Z direction. Because the nanofluids flow in the inlet and the middle section had been subjected to by the Y direction magnetic field, the nanofluids flow in the outlet were turned into a fully developed turbulence and the temperature differences showed the stronger heat transfer performance.

Figure 6 illustrated that the heat transfer coefficients of Cu-H_2O and Al-H_2O nanofluids flow in the circular pipe were affected by magnetic fields. In Figure 6a–c, the magnetic fields were applied along the X, Y, and Z directions, respectively. The diameter of the nanoparticle was 100 nm, and the intensity of magnetic fields was fixed at 0.5T. The results showed that when the magnetic field was applied along the X direction, the heat transfer coefficient of Cu-H_2O nanofluids flow, compared to when no magnetic field was applied, was increased evenly by 9.17%. When the magnetic field was applied along the Y and Z directions, the heat transfer coefficients of Cu-H_2O nanofluids flow were increased evenly by 10.28% and 10.32%, respectively. When the magnetic fields were applied along the Y and Z directions, the heat transfer coefficients of Cu-H_2O nanofluids flow were basically the same, and both were slightly larger than the heat transfer coefficient under the magnetic field in the X direction. The results were consistent with the conclusion drawn from the above study of temperature changes. The reason why the heat transfer coefficient of the nanofluids flow was greater than the X direction by adding the magnetic field in the Y and Z directions was that the magnetic field in the Y and Z directions continuously acts on the middle pipe. When the X-direction magnetic field was applied, the activity of the nanoparticles was weakened because the nanofluids flow in the middle pipe was not disturbed by the Lorentz force, which reduced the chance of collision between particles. The rate of energy exchange was slowed down. Although the magnetic fields continued to be applied to the exit part, the effect was not as good as continuous application.

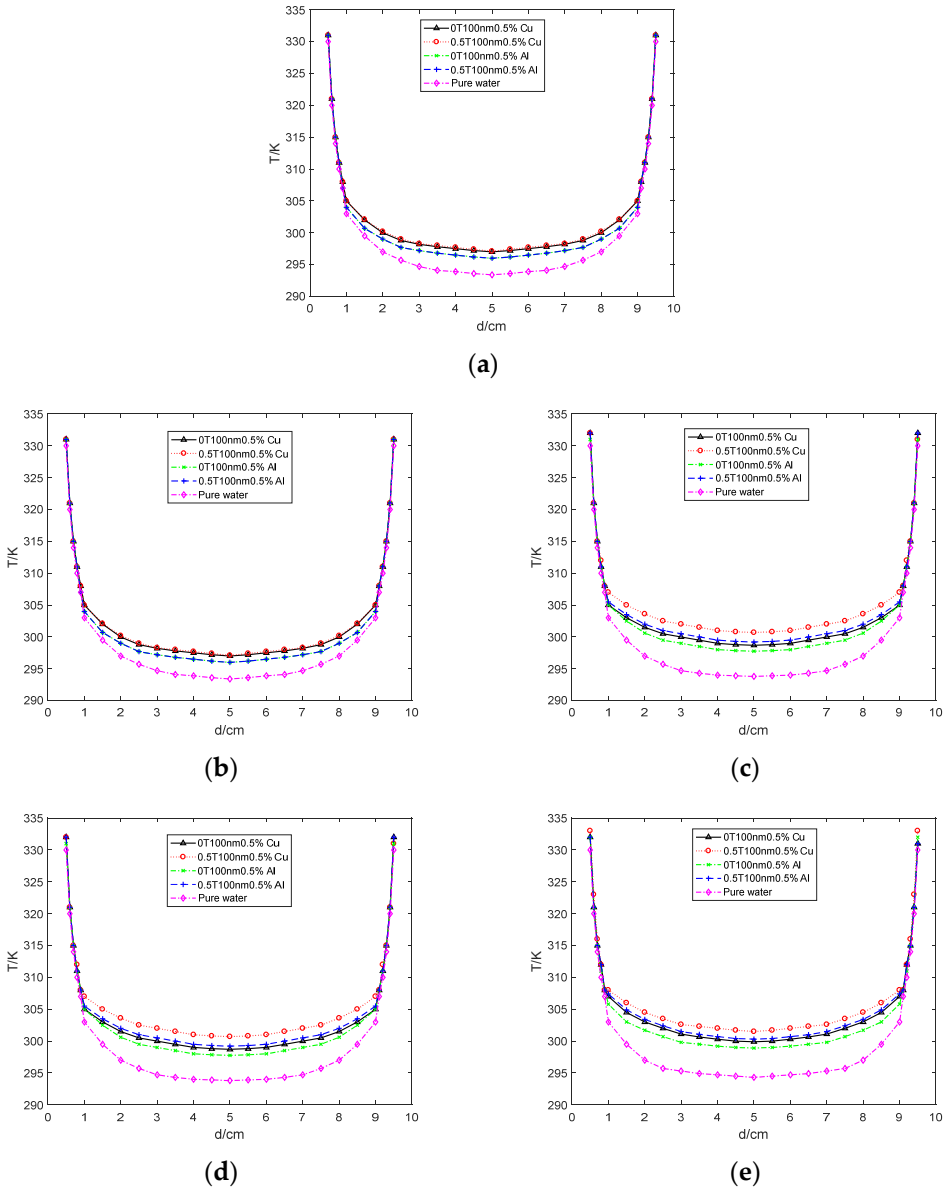

Figure 5. The temperature distributions of Cu-H_2O and Al-H_2O nanofluids flow along the diameter on faces 2 (**a**), 3 (**b**), 4 (**c**), 5 (**d**), and 6 (**e**), respectively. The magnetic fields were applied along the Z direction.

In Figure 6, when the magnetic fields were applied along the X, Y, and Z directions, respectively, the heat transfer coefficients of the Al-H_2O nanofluids flow in the circular pipe were significantly increased. The change trend of the heat transfer coefficients was the same as the Cu-H_2O nanofluids flow, but the heat transfer coefficients of the Al-H_2O nanofluids flow were lower than the Cu-H_2O nanofluids flow. This was because the magnetic susceptibility of Al particles was slightly lower than that of Cu particles. When the diameter of the nanoparticle was 100 nm and the magnetic field was applied along the X direction, the heat transfer coefficient of Al-H_2O nanofluids flow, compared to when no magnetic field was applied, was increased evenly by 8.64%. When the magnetic field was applied along the Y and Z directions, the heat transfer coefficients of Al-H_2O nanofluids flow were increased evenly by 9.66% and 9.68%, respectively.

Appling the magnetic field along the X, Y, and Z axes, respectively, they had a minimally different effect on the heat transfer performance of the nanofluids. The magnetic field along the *X*-axis direction affected the heat transfer performance of the nanofluids less than

the other two directions. The reason for this was that the magnetic field in the X-direction acted intermittently in the middle part, which reduced the activity of the particles and slowed down the energy exchange rate between the particles and the nanofluids, finally decreasing heat transfer performance.

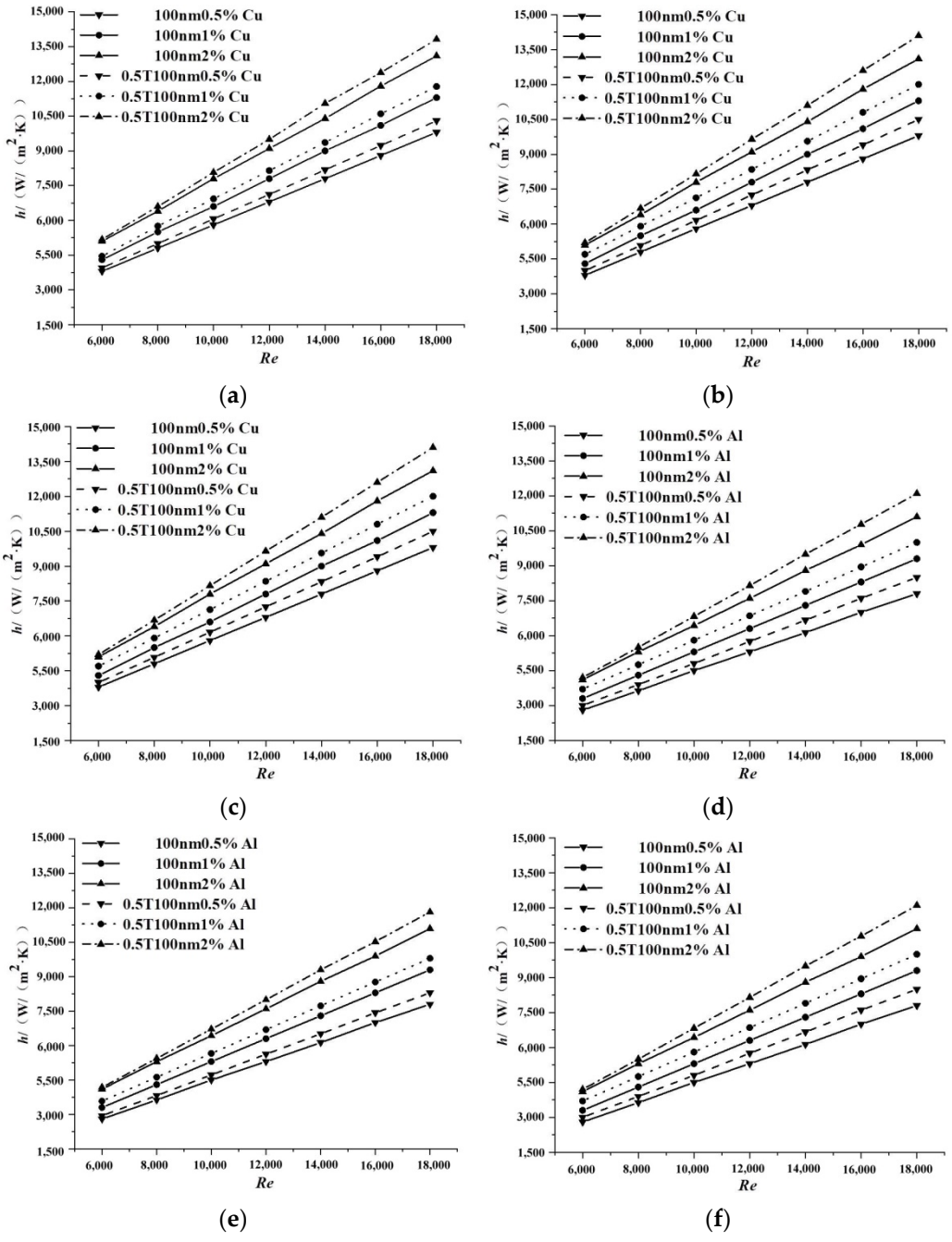

Figure 6. The heat transfer coefficients of Cu-H_2O and Al-H_2O nanofluids flow varied with different Reynolds numbers when the magnetic fields were applied along the X (**a**,**d**), Y (**b**,**e**), and Z (**c**,**f**) directions, respectively.

3.4. Results and Discussions for Different Directions of Magnetic Field

In the previous study, it was mentioned that under a magnetic field in the Y and Z directions, the heat transfer performance enhancement rate of nanofluids were basically the same and maximum. Therefore, in the next simulations, the magnetic field was considered

to be along the Z direction only, when the influence of different intensities of magnetic fields on the forced convection heat transfer of nanofluids flow was discussed.

The heat transfer coefficients of the Cu-H_2O and Al-H_2O nanofluids under different magnetic fields were first explored. Figure 7 illustrated that the heat transfer coefficients of the Cu-H_2O and Al-H_2O nanofluids flow were affected by magnetic fields. When the volume fractions of the Cu-H_2O nanofluids were 0.5% and the intensities of magnetic fields were 0.2 T, 0.5 T, and 0.8 T, the heat transfer coefficients of the Cu-H_2O nanofluids flow were increased evenly by 1.51%, 8.73%, and 10.46%, respectively. The heat transfer coefficients of the Al-H_2O nanofluids flow were increased evenly by 1.69%, 10.16%, and 11.84%, respectively. In Figure 7b, when the volume fractions of the Cu-H_2O nanofluids were 1%, the heat transfer coefficients of the Cu-H_2O nanofluids flow were increased evenly by 1.70%, 8.88%, and 10.26%, and the heat transfer coefficients of the Al-H_2O nanofluids flow were increased evenly by 1.73%, 9.06%, and 10.34%. In Figure 7c, when the volume fractions of the Cu-H_2O nanofluids were 2%, the heat transfer coefficients of the Cu-H_2O nanofluids flow were increased evenly by 1.70%, 7.66%, and 8.26%, and the heat transfer coefficients of the Al-H_2O nanofluids flow were increased evenly by 1.73%, 8.38%, and 8.61%.

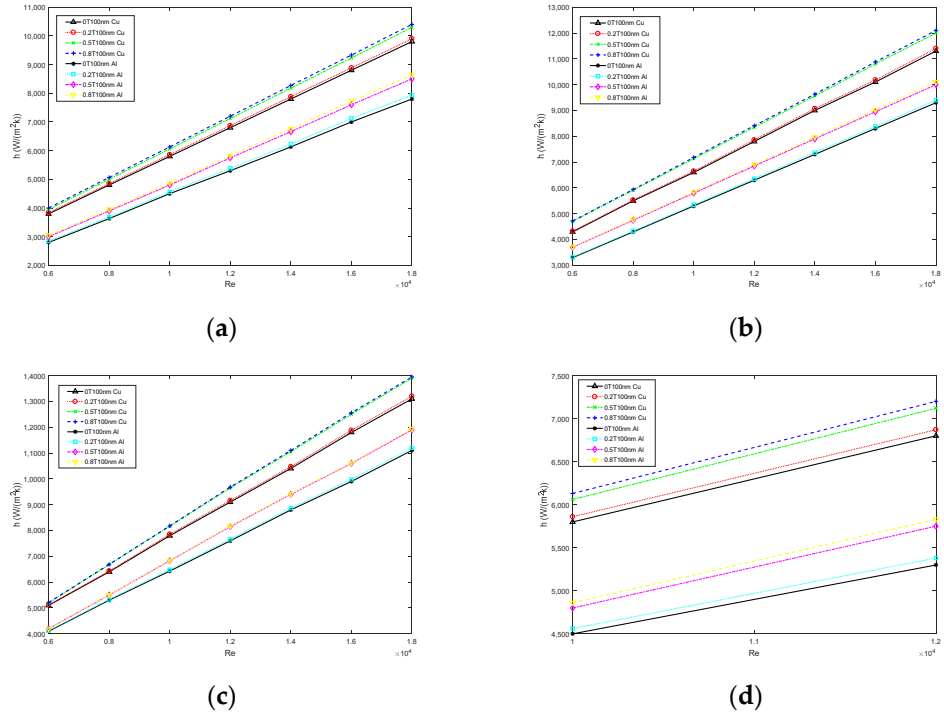

Figure 7. The heat transfer coefficients of the Cu-H_2O and Al-H_2O nanofluids flow varied with different Reynolds numbers. The magnetic fields were applied along the Z direction, and the intensities of magnetic fields were 0.2 T, 0.5 T, and 0.8 T. The volume fractions of nanoparticles were 0.5% (**a**), 1% (**b**), and 2% (**c**). (**d**) Zoom in (**a**) for detail on when Re were 10,000 and 12,000.

The above results showed that the convective heat transfer coefficient of the nanofluid increased with the increasement of the magnetic field intensity. When the magnetic field intensity was 0.2 T, due to the relatively low magnetic susceptibility of metal Cu particles and Al particles, the magnetic field had little effect on the heat transfer performance of the nanofluids, the heat transfer coefficient of the nanofluid did not change much, and the heat transfer of nanofluids was not greatly enhanced. When the magnetic field intensity reached 0.5 T, the heat transfer coefficient of the fluid increased significantly, and the heat transfer performance was significantly enhanced. The magnetic field intensity, at this time, is the most suitable for heat transfer enhancement of nanofluids. When the magnetic field reached 0.8 T, the change in heat transfer coefficient was very small compared with that at

0.5 T, indicating that the influence of the magnetic field on the heat transfer performance of nanofluids had reached the saturation point. Continuing to increase the magnetic field intensity had a small influence on the heat transfer coefficient.

Figure 8 illustrated that the Nusselt number increased non-linearly with the increasement of the magnetic field intensity. Similar to the heat transfer coefficient, low magnetic field intensity had little effect on the Nusselt number of the fluid. In Figure 8, when the magnetic fields were applied along the Z direction, the effects of three different intensities of magnetic fields on the Nusselt numbers of the Cu-H_2O and Al-H_2O nanofluids flow in the circular pipe were illustrated. As Figure 8a,d shows, the Nusselt numbers of the Cu-H_2O nanofluids flow, compared to when no magnetic field was applied, were increased evenly by 1.02%, 6.37%, and 7.14% when the intensities of magnetic fields were 0.2 T, 0.5 T, and 0.8 T, respectively. The Nusselt numbers of the Al-H_2O nanofluids flow were increased evenly by 1.23%, 7.48%, and 8.15%, respectively. In Figure 8b, when the volume fractions of the Cu-H_2O nanofluids was 1%, the Nusselt numbers of the flow were increased evenly by 0.87%, 5.97%, and 6.63%, respectively. The Nusselt numbers of the Al-H_2O nanofluids flow were increased evenly by 0.98%, 6.61%, and 7.15%, respectively. In Figure 8c, when the volume fraction of the Cu-H_2O nanofluids was 2%, the Nusselt numbers of the flow were increased evenly by 0.62%, 5.33%, and 6.14%, respectively. The Nusselt numbers of the Al-H_2O nanofluids flow were increased evenly by 0.81%, 5.48%, and 6.35%, respectively.

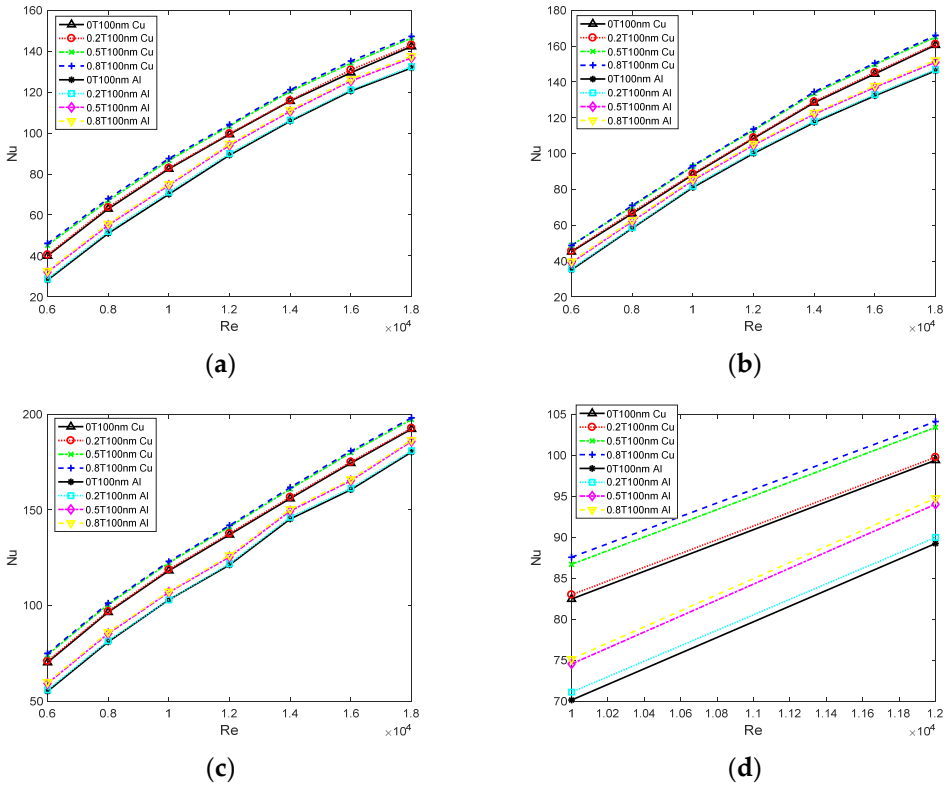

Figure 8. The Nusselt numbers of the Cu-H_2O and Al-H_2O nanofluids flow varied with different Reynolds numbers. The magnetic fields were applied along the Z direction and the intensities of magnetic fields were 0.2 T, 0.5 T, and 0.8 T. The volume fractions of nanoparticles were 0.5% (**a**), 1% (**b**), and 2% (**c**). (**d**) Zoom in (**a**) for details concerning when Re was 10,000 and 12,000.

It was concluded by the above results that the heat transfer coefficients and the Nusselt numbers both were increased with the increment of intensities of the magnetic field. When the intensity of magnetic field was 0.2 T, the heat transfer coefficients and the Nusselt numbers of the nanofluids flow did not change much. The thermal capacity was greatly enhanced. When the intensity of magnetic field reached 0.5 T, the heat transfer coefficients and the Nusselt numbers of the nanofluids flow were significantly increased, and the

heat transfer performance was significantly enhanced. When the intensity of magnetic field increased to 0.8 T, the heat transfer coefficients and the Nusselt numbers were not obviously increased.

4. Conclusions and Outlook

The magnetic fields effects on the heat transfer enhancement were investigated and the magnetic fields were applied by different directions and magnetic field intensities to the flow. In this paper, the diameters of the Cu and Al nanoparticles were 100 nm, 200 nm, and 500 nm, and the volume fractions of the nanofluids were 0.5%, 1%, and 2%. The effects of three different intensities of magnetic fields, 0.2 T, 0.5 T, and 0.8T, on the forced convective heat transfer of the nanofluids flow in the pipe, were studied.

When the magnetic fields were applied along the X, Y, and Z directions, respectively, the temperature distributions, the heat transfer coefficient, and the Nusselt numbers were discussed and compared with the cases without the magnetic field. It was concluded that the temperature difference in the faces of the three sections were increased with the effect of the magnetic field, and the heat transfer coefficient and the Nusselt numbers increased significantly. When the magnetic field was considered to be along Z direction only and the intensity of magnetic fields was fixed at 0.5T. The heat transfer coefficients of Cu-H_2O and Al-H_2O nanofluids flow were increased evenly by 10.32% and 9.68%, respectively, compared with when no magnetic field was applied. Because of a shortage of the pipe length, under the other two directions of magnetic fields, a similar phenomenon was obtained, and the differences between the results were not obvious. When the intensities magnetic fields were 0.2 T, 0.5 T, and 0.8 T, the influences of the magnetic fields on the heat transfer of Cu-H_2O and Al-H_2O nanofluids flow were explored. When the intensity of magnetic field was 0.2 T, because the magnetic susceptibility of metallic Cu nanoparticles and Al nanoparticles was relatively low, this intensity had little effect on the heat transfer performance of the fluid, and the heat transfer capacity was not significantly improved. When the intensity of magnetic field increased to 0.5 T, the heat transfer performances of the two nanofluids flow were effectively improved. When the diameters of the Cu and Al nanoparticles were 100 nm and the volume fractions of the nanofluids was 0.5%, the Nusselt numbers of the Cu-H_2O and Al-H_2O nanofluids flow were increased evenly by 6.37% and 7.48%, respectively. When the intensity of magnetic field increased to 0.8 T, the heat transfer coefficients and the Nusselt numbers did not increase by much.

At present, under the different directions of magnetic fields, a similar phenomenon was obtained because of shortage of the pipe length. Therefore, a two-dimensional numerical simulation work under a magnetic field is necessary and important for long pipe flow. This shall be the subject of future work.

Author Contributions: Conceptualization, Y.Y. and Y.Z.; methodology, K.W.; software, N.D.; validation, Y.Y., K.W. and Y.Z.; formal analysis, K.W.; investigation, K.W.; resources, N.D.; data curation, Q.C.; writing—original draft preparation, Y.Y.; writ-ing—review and editing, Y.Z.; project administration, Q.C.; funding acquisition, Y.Y. All authors have read and agreed to the published version of the manuscript.

Funding: The authors wish to acknowledge the financial support of National Natural Science Foundation of China, NSFC (Grant No. 11702061), and "Thirteenth Five-Year" Science and Technology Project of the Education Department of Jilin Province, (Grant No. JJKH20180437KJ).

Conflicts of Interest: The authors declare no conflict of interest.

References

1. Fu, Q.; Xiao, C.; Huang, Y.; Liao, Q.; Xia, A.; Chen, H.; Zhu, X. Numerical study of flow and heat transfer characteristics of microalgae slurry in a solar-driven hydrothermal pretreatment system. *Appl. Therm. Eng.* **2020**, *164*, 114476. [CrossRef]
2. Blonoga, Y.; Stybel, V.; Maksysko, O.; Drachuk, U. A New Universal Numerical Equation and a New Method for Calculating Heat-Exchange Equipment Using Nanofluids. *Int. J. Heat Technol.* **2020**, *38*, 151–164. [CrossRef]

3. Aminian, A.; Zarenezhad, B. Robust Neuromorphic Model for Simultaneous Prediction of Convection Heat Transfer Coefficient and Friction Factor of Nanofluid Flow in Heat Exchanging Equipment. *J. Numer. Heat Transf. Appl.* **2018**, *73*, 501–516. [CrossRef]
4. Herrera, B.; Gallego, A.; Cacua, K. Experimental Evaluation of a Thermosyphon-based Heat Exchanger Working with a Graphene Oxide (GO) Nanofluid in a Cogeneration System. *Therm. Sci. Eng. Prog.* **2021**, *24*, 100949. [CrossRef]
5. Yan, R.S.; Simpson, J.R.; Bertolazzi, S.; Brivio, J.; Watson, M.; Wu, X.F.; Kis, A.; Luo, T.F.; Walker, A.R.H.; Xing, H.L.G. Thermal Conductivity of Monolayer Molybdenum Disulfide Obtained from Temperature-Dependent Raman Spectroscopy. *ACS Nano* **2014**, *8*, 986–993. [CrossRef]
6. Jin, C.; Wu, Q.B.; Yang, G.Q.; Zhang, H.Y.; Zhong, Y.F. Investigation on Hybrid Nanofluids Based on Carbon Nanotubes Filled with Metal Nanoparticles: Stability, Thermal Conductivity, and Viscosity. *Powder Technol.* **2021**, *389*, 1–10. [CrossRef]
7. Sharma, V.; Okram, G.S.; Verma, D.; Lalla, N.P.; Kuo, Y.K. Ultralow Thermal Conductivity and Large Figure of Merit in Low-Cost and Nontoxic Core-Shell Cu@Cu2O Nanocomposites. *ACS Appl. Mater. Interfaces* **2020**, *12*, 54742–54751. [CrossRef]
8. Nandeppanavar, M.M.; Kemparaju, M.C.; Madhusudhan, R.; Vaishali, S. MHD Slip Flow and Convective Heat Transfer Due to a Moving Plate with Effects of Variable Viscosity and Thermal Conductivity. *Multidiscip. Model. Mater. Struct.* **2020**, *16*, 991–1018. [CrossRef]
9. Hossein, A.M.; Amin, M.; Mohammad, A.N.; Roghayeh, G. A Review of Thermal Conductivity of Various Nanofluids. *J. Mol. Liq.* **2018**, *265*, 181–188.
10. Krishna, V.M.; Kumar, M.S. Numerical Analysis of Forced Convective Heat Transfer of Nanofluids in Microchannel for Cooling Electronic Equipment. *J. Mater. Today Proc.* **2019**, *17*, 295–302. [CrossRef]
11. Zhang, T.; Li, G.X.; Chen, J.; Yu, Y.S.; Liu, X.H. Effect of Wall Heat Transfer Characteristic on the Micro Solid Thruster Based on the AP/HTPB Aerospace Propellant. *Vacuum.* **2016**, *134*, 9–19. [CrossRef]
12. Sinnott, R.K. Heat-Transfer Equipment. In *Coulson and Richardson's Chemical Engineering*; Elsevier: Amsterdam, The Netherlands, 1993; pp. 565–702.
13. Bandaru, S.V.R.; Villanueva, W.; Konovalenko, A.; Komlev, A.; Thakre, S.; Skld, P.; Bechta, S. Upward-facing Multi-nozzle Spray Cooling Experiments for External Cooling of Reactor Pressure Vessels-ScienceDirect. *Int. J. Heat Mass Transf.* **2020**, *163*, 120516. [CrossRef]
14. Amarante, A.; Lanoiselle, J.L. Heat Transfer Coefficients Measurement in Industrial Freezing Equipment by Using Heat Flux Sensors. *J. Food Eng.* **2005**, *66*, 377–386. [CrossRef]
15. Deng, Y.; Jiang, Y.; Liu, J. Liquid Metal Technology in Solar Power Generation-Basics and Applications. *Sol. Energy Mater. Sol. Cells* **2021**, *222*, 110925. [CrossRef]
16. Li, J.; Zhou, J.; Chen, B. Review of Wind Power Scenario Generation Methods for Optimal Operation of Renewable Energy Systems. *Appl. Energy* **2020**, *280*, 115992. [CrossRef]
17. Kowalczyk, T.; Badur, J.; Bryk, M. Energy and Exergy Analysis of Hydrogen Production Combined with Electric Energy Generation in a Nuclear Cogeneration Cycle. *Energy Convers. Manag.* **2019**, *198*, 111805. [CrossRef]
18. Ghorbani, B.; Javadi, Z.; Zendehboudi, S.; Amidpour, M. Energy, Exergy, and Economic Analyses of a New Integrated System for Generation of Power and Liquid Fuels Using Liquefied Natural Gas Regasification and Solar Collectors. *Energy Convers. Manag.* **2020**, *219*, 112915. [CrossRef]
19. Choi, S.U.S. Enhancing Thermal Conductivity of Fluids with Nanoparticles. *J. ASME FED* **1995**, *231*, 99–106.
20. Wang, B.X.; Zhou, L.P.; Peng, X.F. A Fractal Model for Predicting the Effecttive Thermal Conductivity of Liquid with Suspension of Nanoparticles. *Int. J. Heat Mass Transf.* **2003**, *46*, 2665–2672. [CrossRef]
21. Sun, B.; Yan, D.F.; Yang, D. Flow and Heat Transfer Characteristics of Cu-water Nanofluids in Twisted-Tape Inserts in Tubes. *J. Northeast. Dianli Univ.* **2016**, *36*, 74–81.
22. İlhan, B.; Kurt, M.; Ertürk, H. Experimental Investigation of Heat Transfer Enhancement and Viscosity Change of HBN Nanofluids. *Exp. Therm. Fluid Sci.* **2016**, *77*, 272–283. [CrossRef]
23. Karthikeyan, N.R.; Philip, J.; Raj, B. Effect of Clustering on the Thermal Conductivity of Nanofluids. *J. Mater. Chem. Phys.* **2008**, *109*, 50–55. [CrossRef]
24. Liu, C.H.; Qiao, Y.; Du, P.X.; Zhang, J.H.; Zhao, J.T.; Liu, C.Z.; Huo, Y.T.; Qi, C.; Rao, Z.H.; Yan, Y.Y. Recent advances of nanofluids in micro/nano scale energy transportation. *Renew. Sustain. Energy Rev.* **2021**, *149*, 111346. [CrossRef]
25. Zhang, T.J.; Liu, C.C.; Gu, Y.L.; Jérôme, F. Glycerol in Energy Transportation: A State-of-the-art Review. *Green Chem.* **2021**, *23*, 7865–7889. [CrossRef]
26. Liu, C.H.; Yan, Y.; Sun, W.J.; Shi, X.C.; Shi, N.Y.; Huo, Y.X.; Zhao, J.T.; Said, Z.; Sharifpur, M. Preparation and thermophysical study on a super stable copper oxide/deep eutectic solvent nanofluid. *J. Mol. Liq.* **2022**, *356*, 119020. [CrossRef]
27. Liu, C.H.; Sun, W.J.; Huo, Y.X.; Zhao, J.T.; Said, Z. Thermophysical study of glycerol/choline chloride deep eutectic solvent based nanofluids. *J. Mol. Liq.* **2022**, *363*, 119862. [CrossRef]
28. Bahiraei, M.; Hangi, M. Investigating the Efficacy of Magnetic Nanofluid as a Coolant in Double-Pipe Heat Exchanger in the Presence of Magnetic Field. *J. Energy Convers. Manag.* **2013**, *76*, 1125–1133. [CrossRef]
29. Naphon, P.; Wiriyasart, S. Experimental Study on Laminar Pulsating Flow and Heat Transfer of Nanofluids in Micro-Fins Tube with Magnetic Fields. *Int. J. Heat Mass Transf.* **2018**, *118*, 297–303. [CrossRef]
30. Hajmohammadi, M.R.; Haji, M. Effects of the Magnetic Field on the Cylindrical Couette Flow and Heat Transfer of a Nanofluid. *J. Phys. A Stat. Mech. Its Appl.* **2019**, *523*, 234–245. [CrossRef]

31. Selimefendigila, F.; Öztop, H.F. Impacts of using an elastic fin on the phase change process under magnetic field during hybrid nanoliquid convection through a PCM-packed bed system. *Int. J. Mech. Sci.* **2022**, *216*, 106958. [CrossRef]
32. Wang, G.N.; Zhang, Z.; Wang, R.J.; Zhu, Z.F. A Review on Heat Transfer of Nanofluids by Applied Electric Field or Magnetic Field. *Nanomaterials* **2020**, *10*, 2386. [CrossRef] [PubMed]
33. Gnielinski, V.V. Neue Gleichungen fürden Wärme-und den Stoffübergang in turbulent durchströmten Rohren und Kanälen. *J. Forsch. Im Ing. A* **1975**, *41*, 8–16. [CrossRef]
34. Xuan, Y.M.; Li, Q. Investigation on Convective Heat Transfer and Flow Features of Nanofluids. *J. Heat Transf.* **2003**, *125*, 151–155. [CrossRef]
35. Bennia, A.; Bouaziz, M.N. CFD Modeling of Turbulent Forced Convective Heat Transferand Friction Factor in a Tube for Fe3O4 Magnetic Nanofluid in the Presence of a Magnetic Field. *J. Taiwan Inst. Chem. Eng.* **2017**, *78*, 127–136. [CrossRef]